

# 1 **Changing pattern of springtime biomass burning over Peninsular** 2 **Southeast Asia (PSEA) in the recent decade**

3 Saginela Ravindra Babu<sup>1\*</sup>, Neng-Huei Lin<sup>1,2\*</sup>

4 <sup>1</sup>Department of Atmospheric Sciences, National Central University, Taoyuan 32001, Taiwan.

5 <sup>2</sup>Center for Environmental Monitoring and Technology, National Central University, Taoyuan  
6 32001, Taiwan.

7 Correspondence to: S. Ravindra Babu ([baburavindra595@gmail.com](mailto:baburavindra595@gmail.com)) and Neng-Huei Lin  
8 ([nhlin@cc.ncu.edu.tw](mailto:nhlin@cc.ncu.edu.tw)).

## 9 **Abstract:**

10 The focus of this study is to present the recent changes in BB activity over PSEA by considering  
11 decadal changes, 5-year ensemble mean analysis, and long-term trends from twenty years (2001-  
12 2020) of Moderate Resolution Imaging Spectroradiometer (MODIS) active fire counts. The results  
13 revealed that overall springtime BB activity significantly decreased over the past decade (2011-  
14 2020) compared to the previous decade (2001-2010). Surprisingly, the individual monthly analysis  
15 revealed that BB activity over PSEA decreased substantially in March, whereas in April it  
16 increased significantly over the past decade (2011 to 2020). Further, 5-year ensemble means  
17 revealed, BB activity over northern PSEA in March sharply increased during 2006–2010, and  
18 moderately increased in 2011-2015 followed by a profound decrease in 2016-2020. Whereas, in  
19 April, the BB activity showed a pronounced increase in the 2011-2015 and 2016-2020 periods  
20 over northern Laos compared to the rest of PSEA. The observed changes in the BB activity are  
21 strongly reflected in the BB aerosols and gases. The MERRA-2 reanalysis total surface mass  
22 concentration-PM<sub>2.5</sub>, BB black carbon, and MOPITT satellite observed surface carbon monoxide  
23 (CO) showed a significant decrease over northern PSEA in March and a strong enhancement was  
24 evident over northern Laos in April. Finally, the trend analysis in BB activity shows a significant  
25 increasing trend over Laos and Cambodia, and a decreasing trend was found rest of the PSEA.  
26 These findings have important implications for future BB management strategies and regional  
27 climate in the PSEA region.

28 **Keywords:** Biomass burning; Peninsular Southeast Asia; MODIS active fires; Air Pollution  
29

## 30 **1. Introduction**

31 Air pollution is the world's most pressing environmental health crisis and a major contributor to  
32 the global burden of disease (Murray et al., 2020). It is responsible for more than 6.5 million  
33 deaths annually, the bulk of which 70% occurs in the Asia-Pacific region. In addition to health  
34 risks, air pollution poses threats to local economies, food and water security, and the climate  
35 system. (United Nations Environment Programme (UNEP), 2021). Open biomass burning (BB,  
36 including forest, grassland, peat fires, and agricultural waste burning) is one of the major sources  
37 of air pollutants and represents about 30%, 10%, 15%, and 40% of present-day global emissions  
38 of carbon monoxide (CO), nitrogen oxides (NO<sub>x</sub>), black carbon (BC), and organic carbon (OC),  
39 respectively (van Marle et al., 2017; Hoesly et al., 2018; IPCC, 2021). Biomass burning emissions  
40 can influence air quality, radiation, global and regional climate, and ecosystems through aerosol  
41 radiative effects.

42 The Peninsular Southeast Asia (PSEA, including Myanmar, Thailand, Vietnam, Laos, and  
43 Cambodia), is located upstream of the East Asian summer monsoon circulation and is recognized  
44 as one of the key regions affecting the monsoon system and climate (Yang et al., 2021). PSEA is  
45 one of the hotspot regions with the most intensive biomass-burning activities in the world (Reid et  
46 al., 2013; Lin et al., 2013; Lee et al., 2016) and a major contributor of carbon emissions, and  
47 atmospheric aerosols in springtime (March-April). The open BB occurs almost every year during  
48 springtime in the PSEA due to slash-and-burn agricultural activities (Reid et al., 2013; Lin et al.,  
49 2013; Tsay et al., 2016; Huang et al., 2016; 2020; Jainontee et al., 2023) and emits a substantial  
50 amount of aerosols and trace gases into the atmosphere (Ou-Yang et al., 2022; Nguyen et al.,  
51 2022). The BB emissions are responsible for the peaks in aerosol optical depth (AOD), carbon  
52 monoxide, and black carbon during springtime over PSEA (Pani et al., 2018). The BB pollution  
53 from PSEA is often transported from its sources to the East China Sea (ECS), Taiwan, and the  
54 western North Pacific within a few days by the subtropical southwesterly jet and impacts the  
55 downwind air quality, environment, and regional climate (Lin et al., 2009; Lin et al., 2013; Chuang  
56 et al., 2015; Huang et al., 2020; Ou-Yang et al., 2022; Babu et al., 2022).

57 The effects of BB aerosols over the PSEA on regional air quality (Lin et al., 2009; Lin et  
58 al., 2013; Hsiao et al., 2016; Lin et al., 2017; Yang et al., 2022) and climate (Lee et al., 2016; Pani  
59 et al., 2018; Ding et al., 2021; Wang et al., 2021; Li et al., 2022) have been widely investigated

60 based on observations and numerical modeling studies. However, the long-term spatiotemporal  
61 changes and recent trends in the BB activity over PSEA were still limited and not fully explored.  
62 For example, Huang et al. (2016) reported inter-annual variation of springtime BB in PSEA and  
63 its correlation with air quality at Mt. Lulin in Taiwan using long-term (2005–2015) satellite and  
64 global reanalysis data. They found that more (less) springtime BB activity occurred in the years  
65 2007 and 2010 (2005, 2008, 2011, and 2015), respectively. By using 14 years (2003-2016) of  
66 MODIS data, Vadrevu et al. (2019) reported trends in BB activity in South and Southeast Asian  
67 countries and found a statistically-significant increasing trend in BB activity over Cambodia and  
68 Vietnam during the study period. Similarly, Yin et al. (2019) reported detailed seasonal patterns  
69 and tempo-spatial distributions of the different BB types in PSEA by using 16 years (2001-2016)  
70 of MODIS data. A recent Intergovernmental Panel on Climate Change (IPCC) report indicates that  
71 weather conducive to fires has become more frequent in some regions and will continue to increase  
72 with higher levels of global warming (IPCC, 2021). It is necessary to deepen the research and  
73 understanding of the recent changes in BB activity over PSEA. By considering the previously  
74 reported studies, this study for the first time investigates the detailed climatological pattern,  
75 decadal and recent changing patterns, and long-term trends in the BB activity in PSEA over the  
76 past 20 years (2001–2020).

## 77 **2. Data and Methodology**

### 78 **2.1 MODIS active fire products**

79 We used the latest collection of 6.1 Moderate Resolution Imaging Spectroradiometer (MODIS)  
80 active fire products as a proxy for biomass burning activity from January 2001 to December 2020  
81 in the present study. The MODIS on board the Terra (known as Earth Observation Satellite (EOS)  
82 AM-1) and Aqua (known as EOS PM-1) satellites is a key instrument for the identification of fire  
83 activities over the globe (Giglio et al., 2018). MODIS provides information on the geographic  
84 location of the fire spot, fire radiative power (FRP), and fire count detection confidence. MODIS  
85 is one of the most important and longest available data sources of active fire hotspots, providing  
86 the global mapping of fire locations and burned areas. More details and descriptions of the MODIS  
87 fire detection algorithm can be found in Giglio et al. (2018). Each country's Standard Processing  
88 MODIS active fire/hotspot is available online (<https://firms.modaps.eosdis.nasa.gov>; last access:  
89 March 27, 2023).

## 90 **2.2 MERRA-2 Reanalysis products**

91 The Modern-Era Retrospective Analysis for Research and Applications, version 2 (MERRA-2) is  
92 NASA's latest reanalysis dataset and has provided data since 1980; it uses the Goddard Earth  
93 Observing System, version 5 (GEOS-5) Earth system model (Gelaro et al., 2017). It includes the  
94 assimilation of bias-corrected AOD from MODIS and Advanced Very High-Resolution  
95 Radiometer (AVHRR), non-bias-corrected AOD from the space-based Multiangle Imaging  
96 SpectroRadiometer (MISR), and ground-measured AOD from Aerosol Robotic Network  
97 (AERONET) stations (Buchard et al., 2017). We mainly utilized total surface mass concentration-  
98 PM<sub>2.5</sub>, black carbon surface mass concentration, and biomass burning black carbon data,  
99 respectively.

## 100 **2.3 MOPITT carbon monoxide measurements**

101 The surface level carbon monoxide data obtained from the Measurement of Pollution in the  
102 Troposphere (MOPITT, version 8) instrument (Deeter et al., 2019) were also utilized. MOPITT is  
103 a multi-channel Thermal InfraRed (TIR) and Near InfraRed (NIR) instrument operating onboard  
104 the sun-synchronous polar-orbiting NASA Terra satellite. MOPITT V8 CO products, consisting  
105 of a CO profile at ten pressure levels, have been validated; more details about the retrieval  
106 algorithm, validation, and uncertainties of MOPITT CO can be found in Deeter et al. (2019).

107 Apart from the above-mentioned data, we also used the Global Precipitation Climatology  
108 Project (GPCP) Version 3.2 Satellite-Gauge (SG) Combined Precipitation Data Set (Huffman et  
109 al., 2022) and the Global Land Data Assimilation System (GLDAS) soil moisture data (Rodell et  
110 al. 2004).

## 111 **2.4 Methodology**

112 Data confidence in the MODIS fire product is specified by a numeric scale of 0 to 100%.  
113 The active fire hotspots with confidence >30% were only considered in the present analysis. For  
114 the analysis of spatial and temporal variation of BB activity, the daily active fire counts within a  
115 spatial grid of 0.5°×0.5° were aggregated and subsequently averaged for each month over the study  
116 period. Before estimating the trends in BB activity, we obtained the percentage change in BB  
117 activity relative to the respective long-term mean using Eq. 1:

$$118 \quad \text{Relative change in BB activity (\%)} = \left( \frac{x_i - \bar{x}}{\bar{x}} \right) \times 100 \quad (\text{Eq. 1})$$

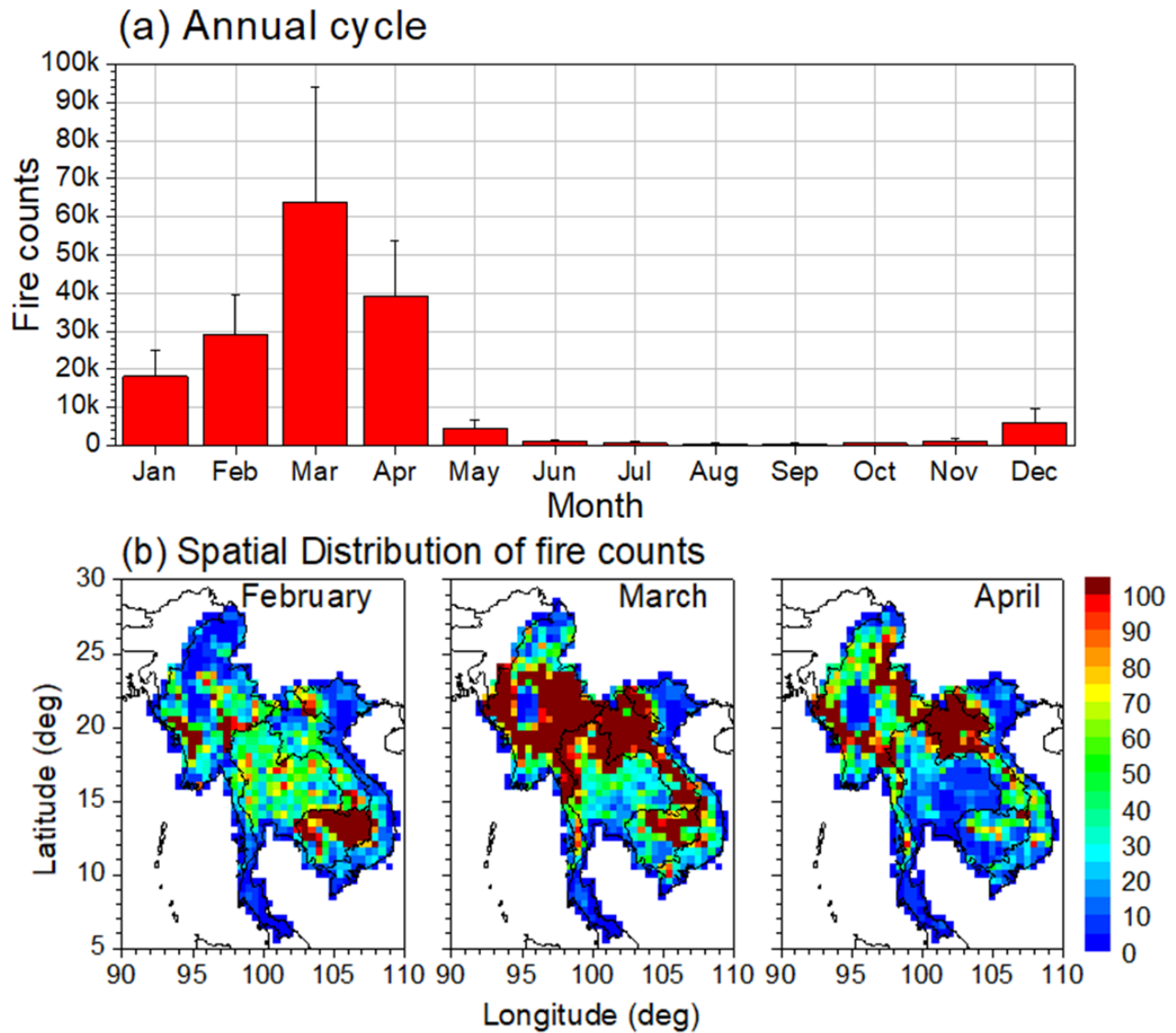
119 where  $x_i$  represents the monthly (annual) mean of the individual month (year), and  $\bar{x}$  is the  
120 corresponding monthly (year) long-term mean calculated using the data from 2001 to 2020.  
121 Finally, the long-term trend in BB activity throughout the observational period has been estimated  
122 using the least-square linear regression trend analysis, and the significance of the trend is tested  
123 using Mann-Kendall tests ( $p < 0.05$ ) (Mann, 1945; Kendall, 1975).

### 124 **3. Results and Discussions**

#### 125 **3.1 Long-term mean structure of springtime Biomass Burning over Peninsular Southeast** 126 **Asia**

127 The long-term MODIS active fire counts were utilized as a proxy for the BB activity over  
128 the PSEA. **Figure 1a** shows the long-term mean annual cycle of the BB activity over PSEA  
129 obtained from MODIS active fire counts averaged between January 2001 to December 2020.  
130 Similarly, **Figure 1b** shows the long-term mean spatial distribution of BB activity from February  
131 through April over PSEA. It is evident from **Figure 1a** that BB activity increases in January  
132 through April, followed by a general decline from May through November. The maximum BB  
133 activity occurred during the springtime and the minimum BB was observed during the summer  
134 monsoon period. The BB activity in summer monsoon months is naturally suppressed due to the  
135 presence of monsoonal rains over the PSEA region. Overall, BB season over the PSEA region  
136 extends from January to April during which more than 70% of total fires are recorded with the  
137 peak during March. Further, the spatial distribution of BB activity from February to April exhibits  
138 quite interesting features over PSEA. The peak BB activity progresses northward in time, and in  
139 February, it was mostly concentrated over Cambodia. Then the BB activity progresses through  
140 Thailand, Laos, and Myanmar, peaking in March and April. It is evident from **Figure 1b** that the  
141 BB activity is higher over northern PSEA than over southern PSEA in both March and April.  
142 Overall, the greatest springtime BB activity occurs in the northern regions of Laos, Cambodia, and  
143 Thailand, eastern and western Myanmar, and lower BB activity in the central regions of Myanmar,  
144 Thailand, and northern Vietnam. The observed long-term mean structure of the BB activity from  
145 the present study is in agreement with the previously reported studies (Vadrevu et al., 2015, 2019;

146 Huang et al., 2020). In the following sections, we mainly focused on BB activity changes and their  
 147 impacts on air quality, and emissions during March and April months only.



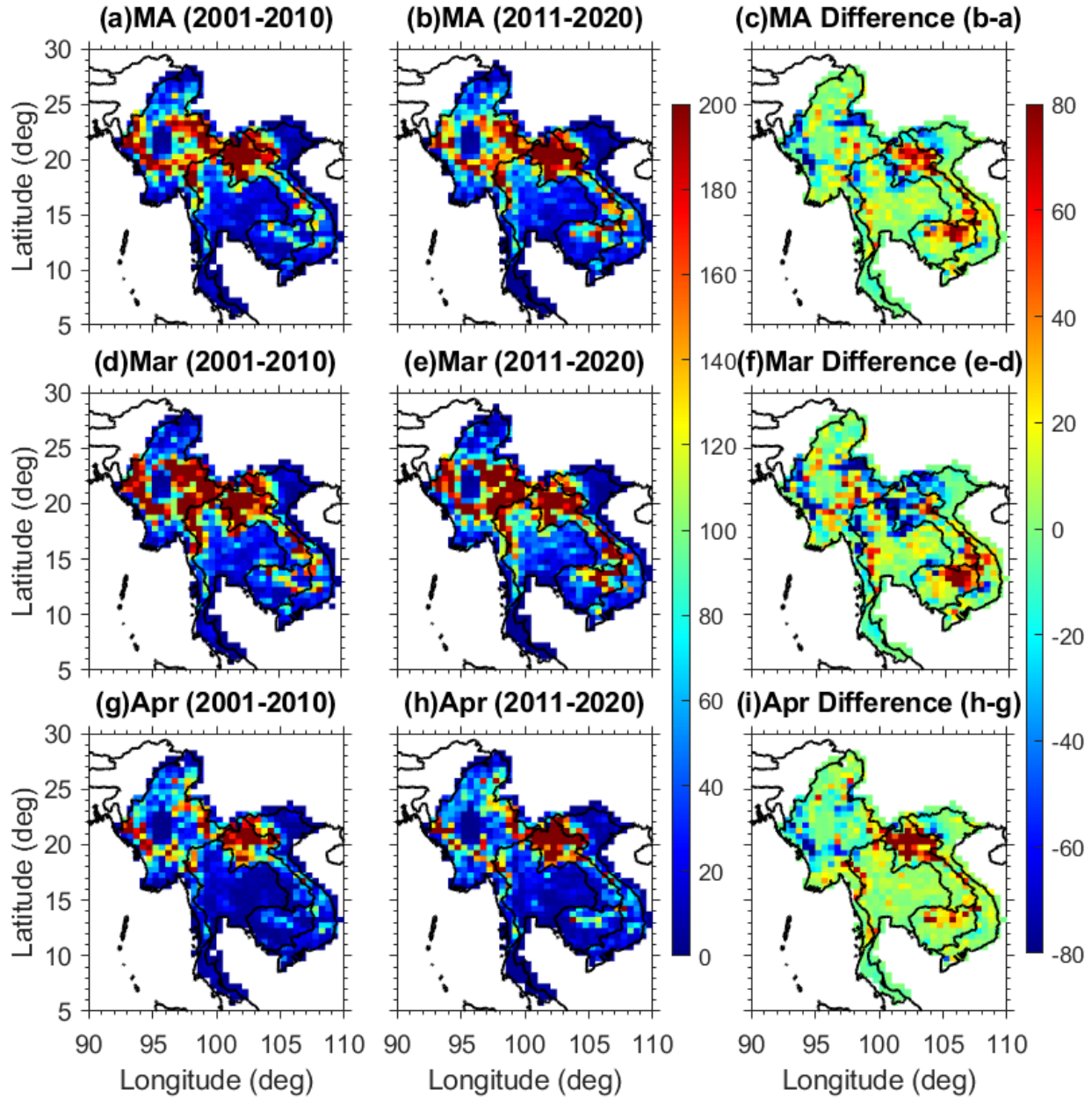
148

149 **Figure 1.** (a) Long-term monthly mean and (b) the spatial distribution of total fire counts in  
 150 February, March, and April months over peninsular Southeast Asia (PSEA) obtained from MODIS  
 151 active fire counts between 2001 to 2020. Vertical error bars shown in subplot (a) indicate  $\pm 1\sigma$   
 152 from the monthly mean.

### 153 3.2 Changing Pattern in Springtime Biomass Burning in Recent Decade

154 The spatial and temporal distribution of BB varies in the tropical region according to forest  
 155 cover and crop residue burning (van der Werf et al. 2017). The long-term MODIS active fire  
 156 products allow producing dense and historical time series of BB activity that can be used to assess

157 the long-term changes in the BB activity over PSEA. To explore the spatiotemporal changes in BB  
 158 activity in PSEA during the past two decades, first, we divided the study period into two periods  
 159 (Decade1: 2001–2010, Decade2: 2011–2020), respectively.



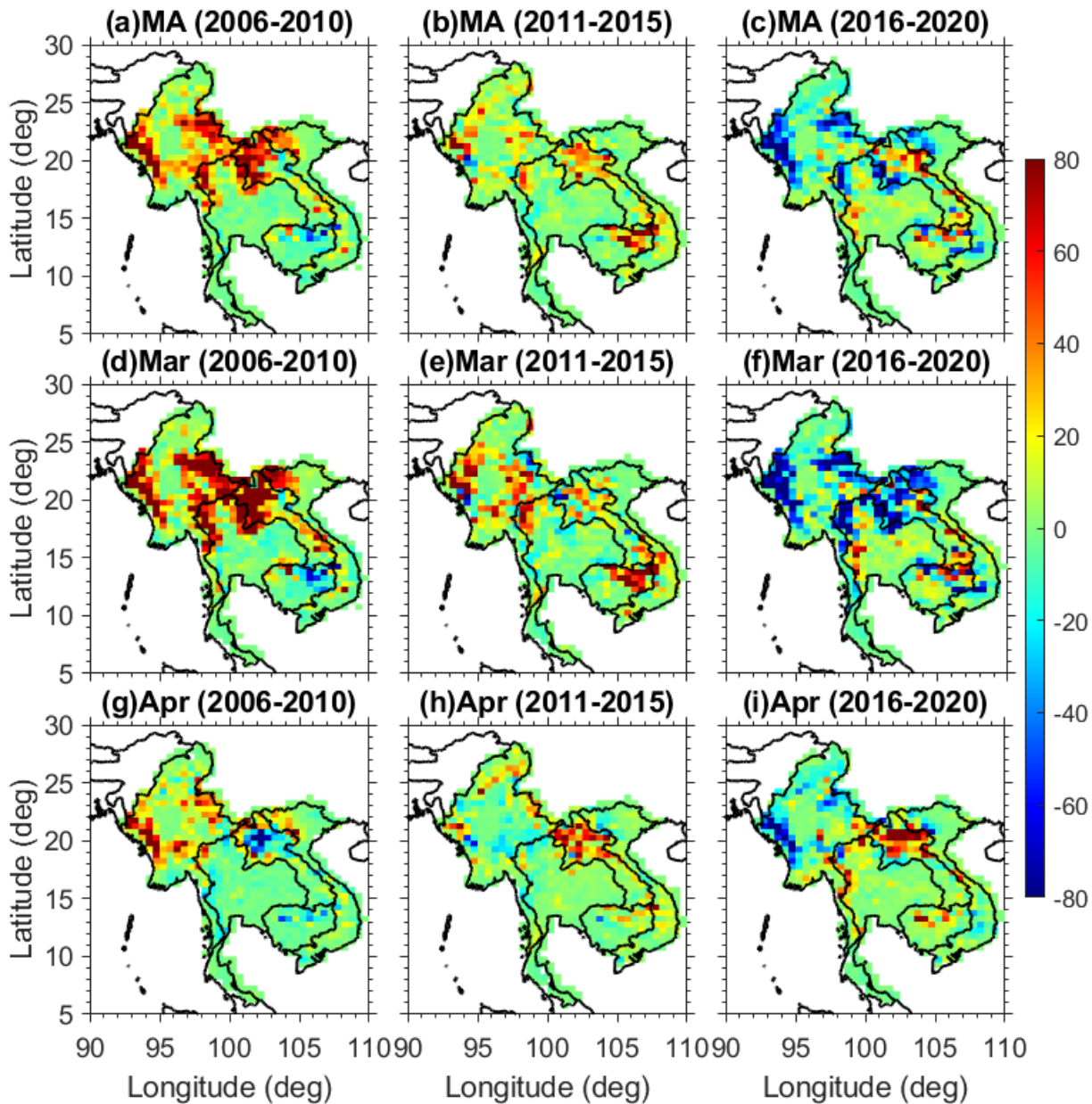
160

161 **Figure 2.** Decadal changes in biomass burning activity over PSEA in springtime (mean of March  
 162 and April), March and April months. To generate this figure, we compared the recent decade 2011-  
 163 2020 active fire counts with the previous decade 2001-2010 (difference of (2011-2020) - (2001-  
 164 2010)).

165 The analysis was carried out for the entire springtime (mean of March and April; hereafter, MA  
166 mean) and individual March and April months, respectively. **Figures 2a-c** show the mean decadal  
167 pattern of the BB activity and the difference between Decade2 and Decade1 in MA mean over  
168 PSEA. Similarly, **Figures 2d-f** and **Figures 2g-i** show the individual months of March and April.  
169 Significant enhancement (decrease) of springtime BB activity was noticed in Decade 2 compared  
170 to Decade 1 over Cambodia and Laos (Myanmar and northern Thailand) (**Fig. 2c**). Individual  
171 monthly analysis revealed distinct results between March and April in Decade 2. Comparing  
172 **Figures 2d-f** and **Figures 2g-i**, we can see that the changes in the BB activity in the recent decade  
173 were not similar in March and April. It is very clear from **Figure 2f** that during March month, the  
174 BB activity significantly decreased over most of the PSEA region except for northeastern  
175 Cambodia and southern Laos where it shows significantly increasing BB activity in Decade 2.  
176 Very interestingly, the difference between Decade2 and Decade1 BB activity in April clearly  
177 shows pronounced increasing BB activity, particularly in northern parts of Laos (**Fig. 2i**). This  
178 discrepancy suggests that the BB activity was higher in April compared to March over north PSEA  
179 during the recent decade and also increased over northeastern PSEA compared to the northwestern  
180 PSEA. This is strongly indicating the shifting of the peak BB activity over PSEA in the recent  
181 decade (2011-2020).

182 To see more clearly the changing pattern of BB activity in recent periods, we further  
183 investigated the BB activity by considering the 5-year ensemble mean anomaly over PSEA. To  
184 quantify the recent changes in BB activity, the 20 years of MODIS active fire data were divided  
185 into four sub-periods: 2001–2005, 2006–2010, 2011-2015, and 2016–2020. Then we obtained the  
186 fire anomalies for four sub-periods based on the background long-term mean (2001-2020) of  
187 MODIS active fires. **Figure 3a-c** shows the observed springtime (MA mean) 5-year ensemble  
188 mean active fire counts anomalies for the 2006–2010, 2011-2015, and 2016–2020 periods.  
189 Similarly, **Figure 3d-f** (**Fig. 3g-i**) shows the observed 5-year ensemble mean active fire counts  
190 anomalies in March (April) for the 2006–2010, 2011-2015, and 2016–2020 periods (figures for  
191 the 2001-2005 period were not shown). Quite opposite patterns were evident between 2006-2010  
192 and 2016-2020 for the springtime BB activity (**Fig. 3a-c**). Substantial enhancement of BB activity  
193 was evident in the 2006-2010 period whereas, a significant lowering of BB activity was evident  
194 during the 2016-2020 period over the north PSEA. The BB activity changes were quite distinct in  
195 March and April over PSEA (**Fig. 3d-i**). During March, the BB activity significantly increased

196 over northern PSEA during 2006-2010 and slightly enhanced between 2011 to 2015, and a  
 197 pronounced decline was found during the 2016-2020 period. However, there was a significant  
 198 increase in BB activity in the recent two periods (2011-2015 and 2016-2020) over south Laos and  
 199 northeastern Cambodia (longitude: 105–107°E latitude: 14–18°N) during March.



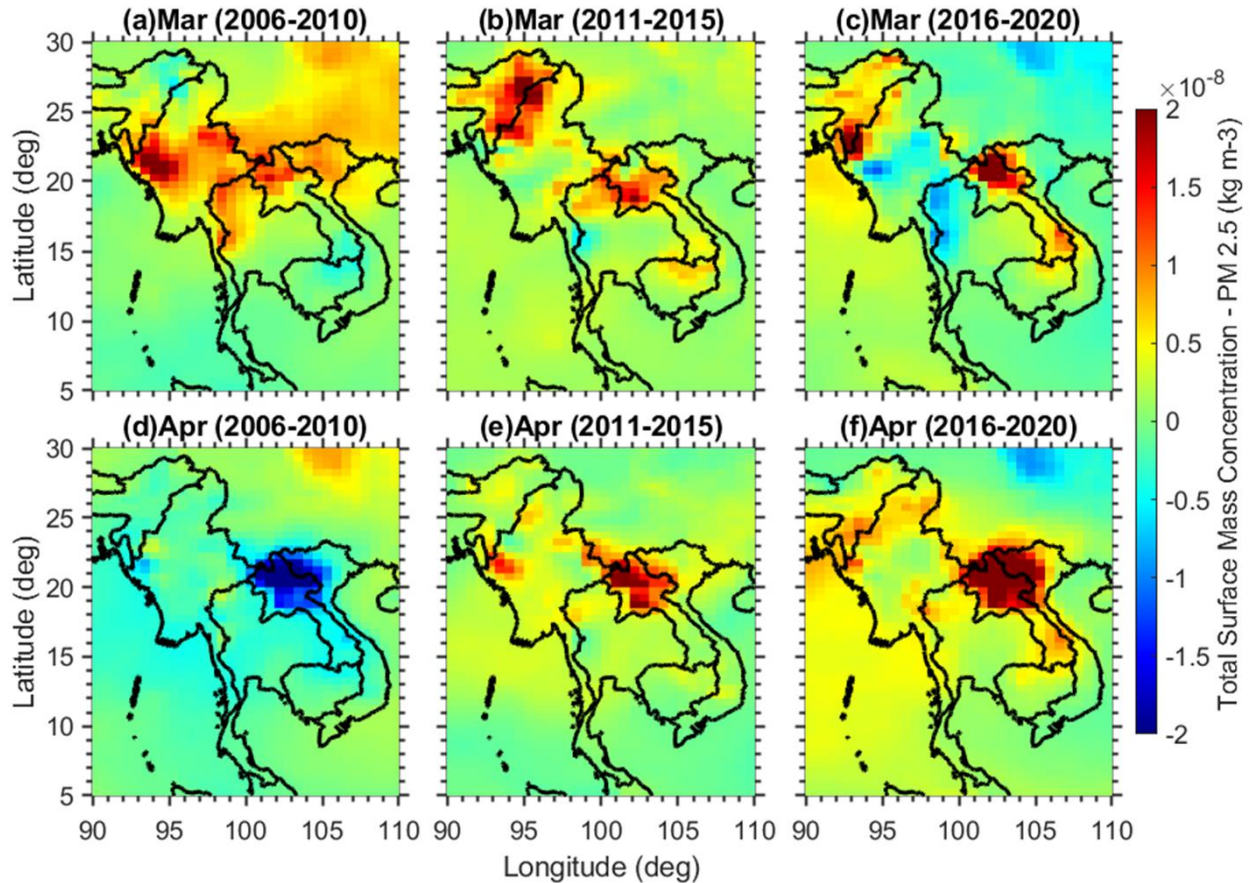
200  
 201 **Figure 3.** Observed MODIS active fire count anomalies compared to the long-term mean (2001-  
 202 2020) in (a) 2006–2010, (b) 2011–2015, and (c) 2016–2020 for springtime (mean of March and  
 203 April). The subplots d-f and g-i are the same as subplots a-c, but for the individual months of  
 204 March and April, respectively.

205 In contrast to March, quite interesting changes were observed in BB activity during April  
206 in recent periods over PSEA. For example, Myanmar shows increased BB activity during 2006-  
207 2010, whereas it shows significantly decreasing BB activity during the recent 2016-2020 period.  
208 Similarly, northern Laos exhibited lowered BB activity during the 2006-2010 period. However,  
209 significant enhancement of BB activity was evident over northern Laos (longitude: 100–105°E  
210 latitude: 18–22°N) in recent two periods (2011-2015 and 2016-2020) compared to the remaining  
211 regions in the PSEA. In conclusion, the dipole pattern of increasing (decreasing) BB activity over  
212 southern PSEA (northern PSEA) during March and increasing (decreasing) BB activity over  
213 northeastern PSEA, particularly Laos (northwestern PSEA) during April was noticed in recent two  
214 periods (2011-2015 and 2016-2020), respectively. Overall, it is clear from **Figures 2** and **3** that  
215 compared to the remaining regions in the PSEA, Laos, and Cambodia become hotspot regions for  
216 peak BB activity in the recent decade. These changes in the BB activity in the recent period may  
217 affect local air quality, carbon emissions, and regional climate. It may be worthwhile to investigate  
218 further how these unusual changes in BB activity reflect on the distribution of BB aerosols and  
219 carbon gases over the PSEA during recent periods. Hence, we further examined the total surface  
220 mass concentration-PM<sub>2.5</sub>, BB-black carbon, and carbon monoxide changes that are associated  
221 with the change of BB activity in recent periods over PSEA. The detailed results are further  
222 discussed in the following sections, respectively.

### 223 **3.3 Impact of Changing BB Pattern on BB Aerosols and Carbon Emissions**

224 It is well known that BB emissions are major sources of aerosols, greenhouse gases, and  
225 particulate matter over PSEA during the respective peak BB season. For example, it is reported  
226 that the contribution of non-BB AOD was usually lower than that of BB AOD during the  
227 springtime at Chiang Mai Met Station (18.77°N, 98.97°E, 312 m a.s.l.) (Pan et al., 2020) and at  
228 Chiang Mai University (CMU; 18.795°N, 98.957°E, 373 m a.s.l.) (Pani et al., 2018) Thailand in  
229 northern PSEA. Recently, Thao et al. (2022) found that open BB was the largest emission source  
230 in PSEA, contributing 57% to the PM<sub>2.5</sub> concentrations during the peak BB period in March 2012.  
231 For the same period (March 2012), Thao et al. (2022) estimated open BB emission contributes  
232 70% to PM<sub>2.5</sub> concentrations in Laos, followed by Myanmar (69%), Cambodia (54%), Thailand  
233 (47%), and Vietnam (31%). Even some studies based on simulations found that BB aerosols  
234 accounted for up to 90 % of the near-surface PM<sub>2.5</sub>, BC, and OC concentrations over the BB source

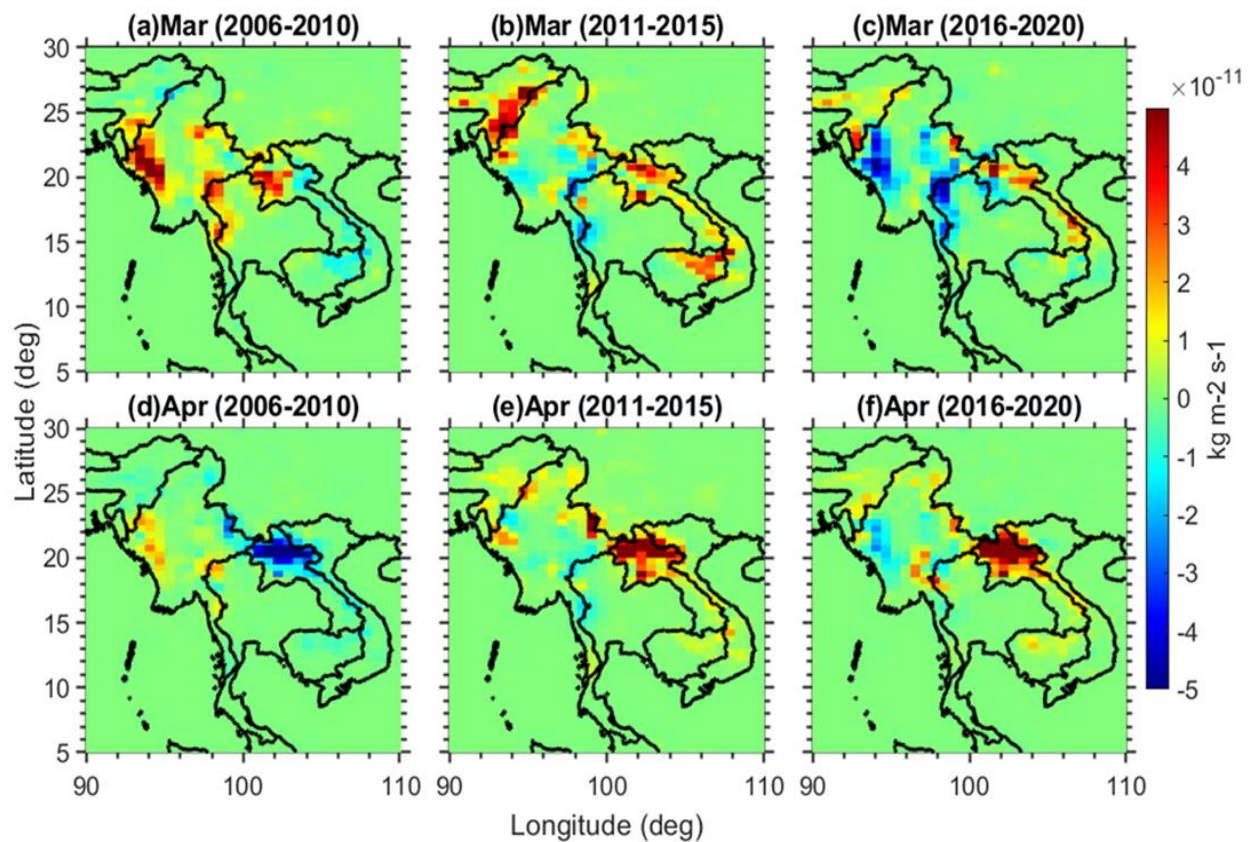
235 regions of north PSEA (Li et al., 2022). Overall, it is clear that BB activity is a major source of air  
 236 pollutants, particulate matter, carbon emissions, and carbonaceous aerosols over PSEA during  
 237 springtime.



238  
 239 **Figure 4.** MERRA-2 reanalysis measured total surface mass concentration-PM 2.5 anomalies  
 240 compared to the long-term mean (2001-2020) in (a) 2006–2010, (b) 2011–2015, and (c) 2016–  
 241 2020 for March month. The subplots d-f are the same as subplots a-c, but for the month of April,  
 242 respectively.

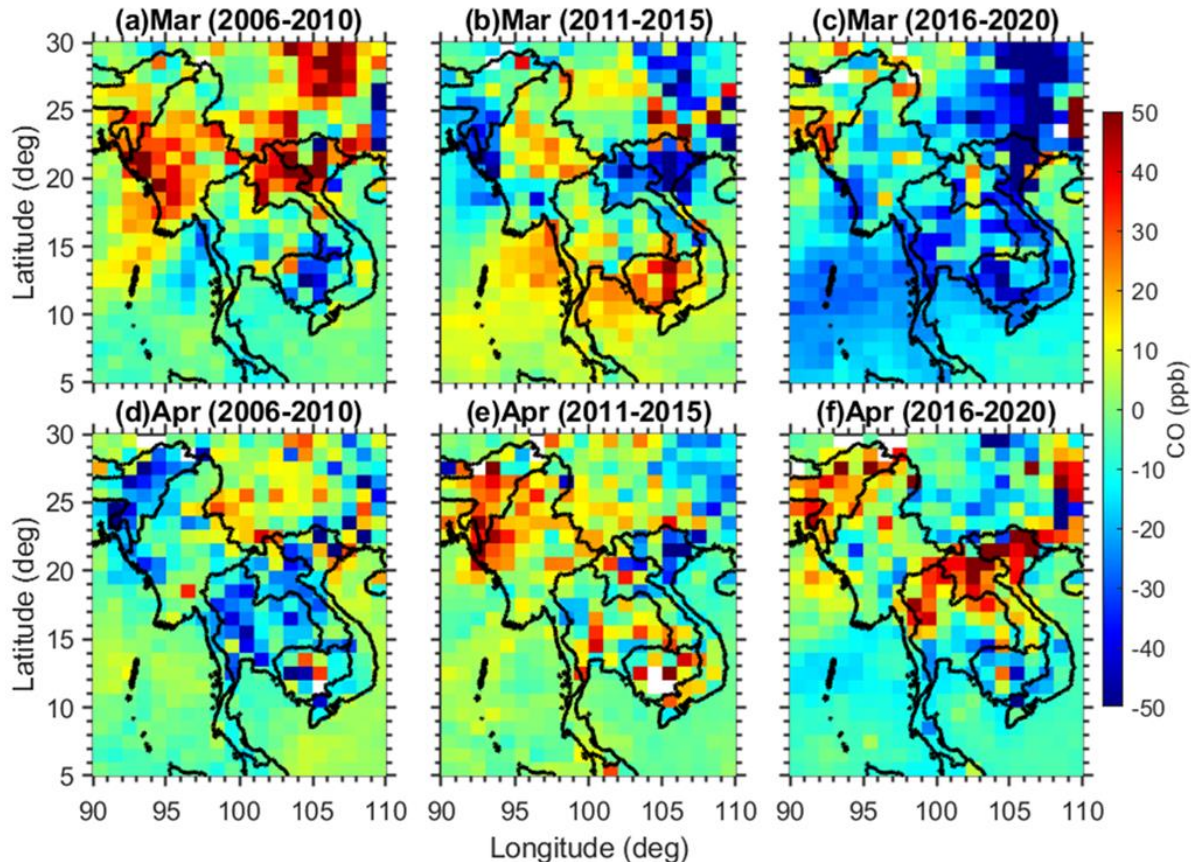
243 We analyzed MERRA-2 reanalysis total surface mass concentration-PM<sub>2.5</sub>, BB black  
 244 carbon, and MOPITT satellite observed surface carbon monoxide (CO) data from 2001-2020  
 245 during springtime to investigate whether similar patterns exist relative to the recent unusual  
 246 changing pattern in BB activity. A similar 5-year ensemble mean analysis was applied to each BB  
 247 aerosol (PM<sub>2.5</sub> and black carbon) and CO, as shown in **Fig. 3**. The 5-year ensemble mean anomaly  
 248 compared to the background long-term mean (2001-2020) in the MERRA-2 measured total surface  
 249 mass concentration- PM<sub>2.5</sub> and BB black carbon are shown in **Figures 4-5**, respectively. Similarly,  
 250 the surface CO anomalies obtained from MOPITT data are shown in **Figure 6**. In 2006–2010

251 during March, the PM<sub>2.5</sub> concentrations, BC, and surface CO in northern parts of PSEA increased  
 252 substantially. Whereas, in 2016-2020, the opposite pattern was noticed as observed in the BB  
 253 activity shown in **Figure 3**, respectively. Interestingly, during April significant positive anomalies  
 254 in the elevated BC (CO) and higher PM<sub>2.5</sub> are observed over northern Laos in recent two periods  
 255 (2011-2015 and 2011-2020) and lowered in 2006-2010, coinciding with the BB anomalies seen in  
 256 **Fig. 3**. The rapid increase in BB activity in April over northern Laos might be one of the possible  
 257 causes of enhanced aerosol loading over this region. The observed increased and decreased PM<sub>2.5</sub>,  
 258 BC, and CO over PSEA in recent decade, strongly supports the observed changes in the BB activity  
 259 over the PSEA. Overall, the substantial changes in the BB activity and BB aerosols changes show  
 260 good agreement over PSEA. Overall, it is clear from the present study that there are significant  
 261 changes in the BB activity over PSEA in the recent decade and Laos become one of the major  
 262 hotspot regions for the peak BB activity and BB emissions in the recent decade.



263  
 264 **Figure 5.** MERRA-2 biomass burning black carbon anomalies compared to the long-term mean  
 265 (2001-2020) in (a) 2006–2010, (b) 2011–2015, and (c) 2016–2020 for March month. The subplots  
 266 d-f are the same as subplots a-c, but for the month of April, respectively.

267

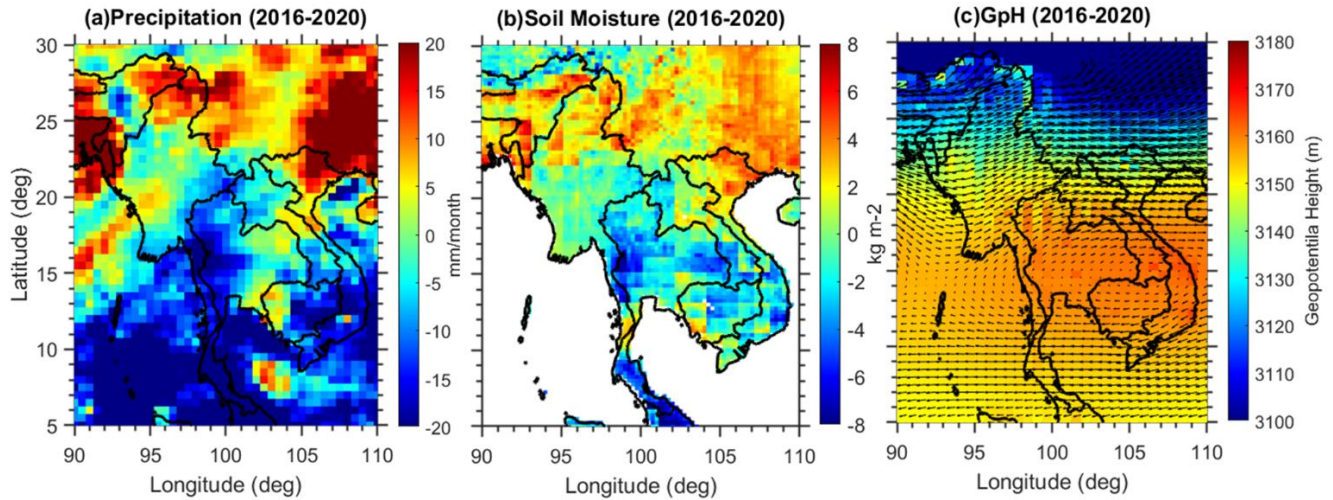


268  
 269 **Figure 6.** MOPITT observed surface carbon monoxide anomalies compared to the long-term mean  
 270 (2001-2020) in (a) 2006–2010, (b) 2011–2015, and (c) 2016–2020 for March month. The subplots  
 271 d-f are the same as subplots a-c, but for the month of April, respectively.

### 272 3.4 Role of Meteorological conditions on recent changes in the BB activity over PSEA

273 The springtime BB activity over PSEA is mostly due to anthropogenic and human origin  
 274 (Vadrevu et al., 2019). However, the local meteorological (precipitation and temperature)  
 275 conditions and atmospheric circulations also can have an impact on changing the BB activity  
 276 (Huang et al., 2016; Vadrevu et al., 2019; Huang et al., 2020). A previous study by Vadrevu et al.  
 277 (2019) suggested that precipitation has a significant correlation compared to the temperature with  
 278 monthly fire counts over PSEA. They concluded that precipitation can explain more variations in  
 279 fires than temperature and precipitation could be explained 40% of fire variations in Thailand,  
 280 41% in Vietnam, and 38% in Cambodia, respectively. Hence, we investigated the precipitation  
 281 changes in the recent period (2016-2020) over PSEA to see the plausible link between substantial  
 282 changes in the BB activity over PSEA. We utilized precipitation data from the Global Precipitation  
 283 Climatology Project (GPCP) Version 3.2 Satellite-Gauge (SG) Combined Precipitation Data Set  
 284 (Huffman et al., 2022). As Soil moisture is also one of the major drivers of BB activity (Hou and

285 Orth, 2020), we also investigated soil moisture changes over PSEA from the Global Land Data  
 286 Assimilation System (GLDAS) data (Rodell et al. 2004). Precipitation and soil moisture anomalies  
 287 are defined as a deviation from the long-term mean of springtime (2001–2020).



288

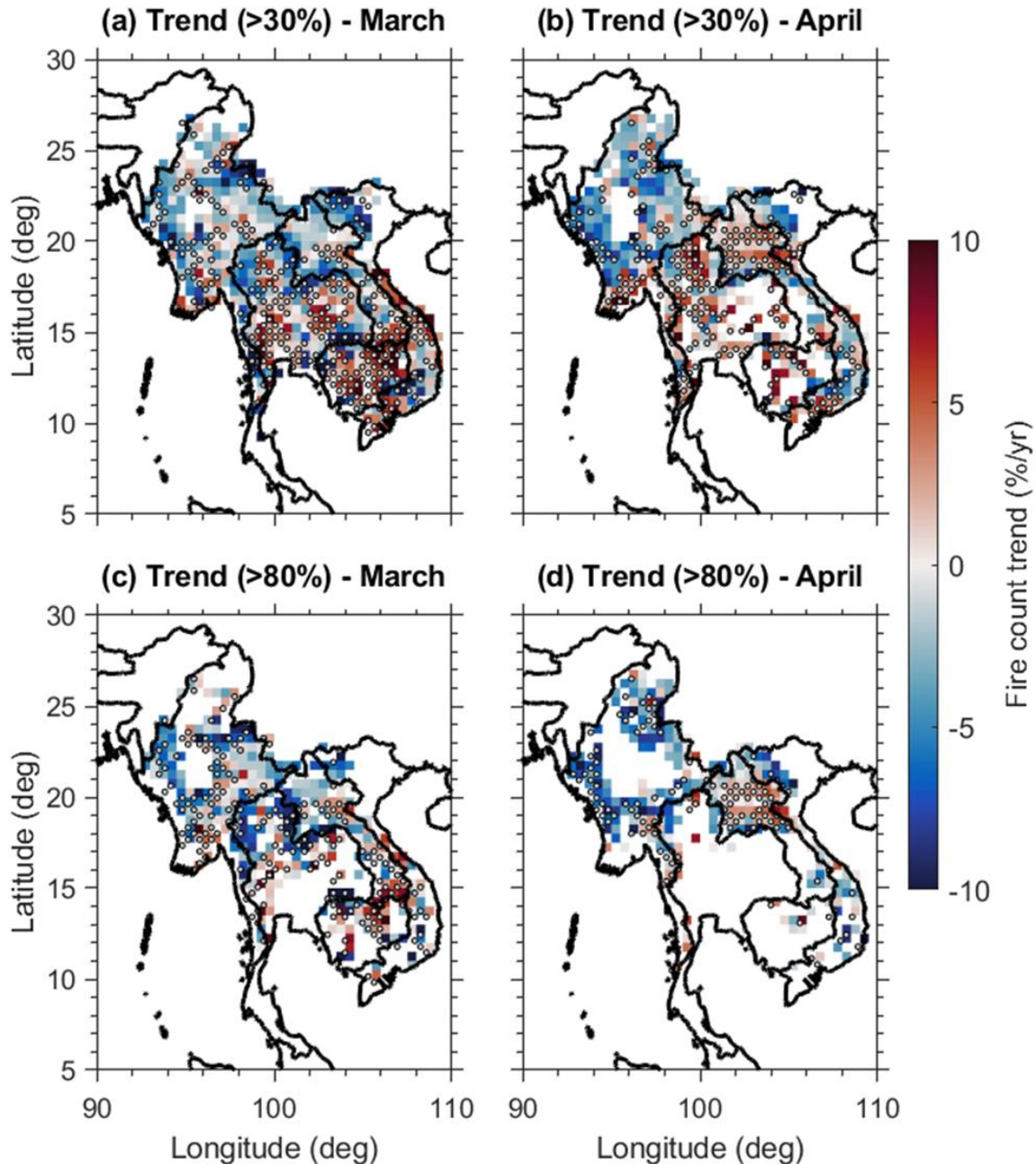
289 **Figure 7.** Springtime (average of March-April) (a) Combined satellite-gauge precipitation  
 290 anomalies and (b) Soil moisture anomalies observed during 2016-2020 compared to the long-term  
 291 mean (2001-2020). Subplot (c) shows MERRA-2 reanalysis measured 700 hPa winds along with  
 292 Geopotential Height observed during the 2016-2020 period.

293 **Figures 7a and 7b** show the precipitation and soil moisture anomalies compared to the  
 294 long-term mean (2001-2020) in the 2016-2020 period over PSEA. The precipitation and soil  
 295 moisture increased over Myanmar during the 2016-2020 period. The enhanced precipitation and  
 296 soil moisture over Myanmar is consistent with the decreased BB activity in the 2016-2020 period.  
 297 Similarly, less precipitation and decreased soil moisture are observed over Cambodia and Thailand  
 298 during the 2016-2020 period, consistent with the observed BB activity shown in **Fig. 3**. The  
 299 lowered precipitation and drier soil over Cambodia and Thailand are in line with the observed  
 300 anticyclone circulation and increased geopotential height during the 2016-2020 period (**Fig. 7c**).  
 301 This anticyclone over southern PSEA (particularly over Cambodia and Thailand) can induce local  
 302 downdraft, suppresses springtime precipitation (**Fig. 7a**) and provide favorable conditions  
 303 (reducing cloud cover and strong incoming solar radiation) for BB activity. There are some  
 304 additional factors, such as land use change (Reid et al., 2013), government control policies, and  
 305 shifting cultivation that might be involved in the recent changes in BB activity PSEA. For example,  
 306 the decrease in BB activity during March in Thailand from 2016 may have been partially caused  
 307 by Thailand's new air pollution control measures (Yabueng et al., 2020). Whereas, the significant

308 enhancement of peak BB activity in April (particularly during 2011-2015 and 2016-2020) over  
309 northern Laos might be due to the increase in the shifting cultivation in Laos in recent years.  
310 Shifting cultivation is one of the major drivers of forest degradation in Laos (Messerli et al., 2009).  
311 Our findings on the profound increase in BB activity in Laos in recent periods (2011-2015 and  
312 2016-2020) are partially supported by a recent study by Chen et al. (2023). Based on Landsat time  
313 series images from 1991 to 2020 on Google Earth Engine, Chen et al. (2023) monitored the shifting  
314 of cultivation across Laos. They found that the area of slash-and-burn activities in Laos increased  
315 in the 2015–2020 period. It can be noted that the results of Chen et al. (2023) are based on annual  
316 maps from Landsat images but our results from the present study are primarily based on springtime  
317 (March and April) BB activities determined from the number of daily MODIS active fire counts,  
318 respectively. It is also noted that our results are significantly distinct from the findings of Chen et  
319 al. (2023) that a significant increase of BB activity was observed over the northern Laos region in  
320 April compared to March. For instance, the detailed inter-annual variability of springtime BB  
321 activity over PSEA and the effects of various climate teleconnections such as El Niño-Southern  
322 Oscillation (ENSO) and Indian Ocean Dipole (IOD) were excluded from the study. The plausible  
323 relationship between various climate teleconnections and springtime BB activity over PSEA may  
324 be considered in future communication, respectively.

### 325 **3.5 Long-term Trends in Springtime BB Activity over PSEA**

326 Finally, we estimated the long-term trends in BB activity over PSEA. To identify the spatial  
327 pattern in BB activity trend from MODIS active fires over PSEA, we have performed spatial trend  
328 analysis by using linear regression and detected its corresponding significance level based on the  
329 MK method. As the detection confidence of MODIS active fires ranges from 0-100%, above 30%  
330 is considered to have better accuracy (Giglio et al., 2018). Therefore, first, we performed a trend  
331 analysis for the MODIS active fires that are having more than 30% confidence levels. The greater  
332 than 80% confidence levels in the MODIS fires can represent the intense BB activity hence we  
333 also did trend analysis separately for the MODIS fire counts that have greater than 80% confidence  
334 levels.



335

336 **Figure 8.** Long-term trends in the fire activity based on >30% fire counts over PSEA in (a) March,  
 337 and (b) April. The subplots c and d are the same as subplots a and b, but the trends are based on  
 338 >80% fire counts. The dots represent the statistical significance of the estimated trends at 99%  
 339 (0.01 significance level).

340 The trend analysis results for the period 2001-2020 are shown in **Fig. 8**, where the pixels at a 99%  
 341 significant level ( $p < 0.01$ ) are marked with dots. **Figures 8a** and **8c** (**Figures 8b** and **8d**) show the  
 342 observed percentage change in the BB activity trend for March (April). The trend analysis revealed  
 343 a significant increasing trend in BB activity during April that was primarily concentrated in

344 northern Laos. Whereas in March, most of the increasing trend was located over northeastern  
345 Cambodia, respectively. Overall, northeastern Cambodia during March and northern Laos during  
346 April, have increased BB activity by over 10% in the past two decades. The increasing trend in the  
347 BB activity over northern Cambodia during March from the present study is in line with the results  
348 of Vadrevu et al. (2019), who also find a statistically significant increasing trend in the fire activity  
349 over Cambodia from the 2003-2016 period. It is noted that we estimated the BB trends based on  
350 individual March and April months in the present study whereas Vadrevu et al. (2019) estimated  
351 the trends based on annual scales by considering an entire country average of total fire counts. It  
352 is also noted the substantial increasing trend in BB activity over northern Laos, particularly in  
353 April was not reported in Vadrevu et al. (2019). It is also noted that a significant decreasing trend  
354 in BB activity was evident largely aggregated in Myanmar and northern Thailand during March.  
355 It is clear from the decadal changes (**Fig. 2**), the 5-year ensemble mean BB activity changes (**Fig.**  
356 **3**), and long-term trends (**Fig. 8**) that a shift in the distribution of peak BB activity from March to  
357 April was evident over northern PSEA and Myanmar/northern Thailand to northern Laos in the  
358 recent decade (2011-2020). Given the strong importance of springtime BB aerosols on climate,  
359 our present results can contribute significantly further to understanding the long-term changes in  
360 BB activity and associated emissions over PSEA.

#### 361 **4. Summary and Concluding Remarks**

362 Peninsular Southeast Asia (PSEA), particularly the northern part (or region) is confronted with the  
363 problem of air pollution due to widespread biomass burning activity in nearly every dry season  
364 from January to April which has profound effects on tropospheric chemistry and composition in  
365 the East Asian periphery. We have used long-term MODIS active fire counts to characterize the  
366 long-term trends in biomass burning activity and its recent changing pattern over the PSEA for the  
367 past two decades (2001-2020). We also investigated the impact of observed BB activity changes  
368 on BB aerosols and carbon gases by utilizing MERRA-2 reanalysis products and MOPPIT satellite  
369 measurements of surface carbon monoxide. The monthly distribution shows the greatest BB  
370 activity during the dry season from January to April, with its peak in March. Results from the  
371 present study highlight the BB activity distribution, pattern, and recent trends in PSEA which are  
372 important in addressing the regional BB activity and emission issues in PSEA. The major findings  
373 obtained from the study are summarized below:

- 374 • Decadal analysis reveals a significant decrease in BB activity in March in most PSEA  
375 regions over the past decade (2011-2020) and a significant increase in BB activity in April  
376 in northern Laos.
- 377 • Five-year ensemble means anomalies in the BB activity reveals, both decreasing and  
378 increasing BB activity in PSEA were evident in the recent five-year period (2016-2020),  
379 with a dominance of decreasing (increasing) BB activity over Myanmar and northern  
380 Thailand (Laos) in both March and April.
- 381 • In March, statistically significant decreasing BB activity was found over Myanmar and  
382 northern Thailand, whereas, increasing BB activity was evident over northeastern  
383 Cambodia and south Laos.
- 384 • In April, BB activities increased significantly over Laos in the most recent 5-year period  
385 (2016-2020) and the stronger increase was evident over northern Laos.
- 386 • During 2006–2010, northern PSEA experienced the most severe BB activity, with the  
387 highest mean  $PM_{2.5}$  concentrations in most regions. By contrast, during 2016–2020, BB  
388 activity was at its lowest over northern PSEA, with the lowest mean  $PM_{2.5}$  values.
- 389 • BB aerosol ( $PM_{2.5}$  and BC) and carbon monoxide (CO) showed a significant increase in  
390 northern Cambodia and northern Laos over the past decade.
- 391 • Long-term trend analysis revealed a significant increasing trend in PSEA that was  
392 primarily concentrated in Laos during April and Cambodia during March.

393 In light of the end of the MODIS instruments, our present work based on two decades of  
394 data can give an overall overview of the spatial distribution of BB activity and its recent changes  
395 along with the long-term trends over PSEA. Our study also highlighted that Laos has become a  
396 hotspot region for the rapid increase of BB emissions. Based on recent world air quality reports,  
397 there is a severe lack of ground-level monitoring of outdoor ambient  $PM_{2.5}$  in Laos (World Air  
398 Quality Report, 2021/ [https://www.iqair.com/newsroom/WAQR\\_2021\\_PR](https://www.iqair.com/newsroom/WAQR_2021_PR)). Also, it was reported  
399 that the highest health risk rates per 100,000 populations due to open BB to human health were  
400 found in Laos when compared to the rest of the PSEA region (Thao et al., 2022). Similarly, the  
401 results obtained from the present study also suggest more effective measures should be taken to  
402 control BB emissions and stringent policies should be introduced to control the increasing trend  
403 of BB activity in Laos. Overall, our results will help address the issues of BB activity management

404 and pollution, air quality monitoring, and mitigation in the PSEA region. We strongly believe that  
405 the present results can significantly contribute to a better understanding of spatial and temporal  
406 distributions of BB activity and BB aerosol changes over the PSEA.

#### 407 **Competing Interest**

408 The authors declare that they have no conflict of interest.

#### 409 **Data availability**

410 The MODIS fire products can be downloaded from  
411 [https://firms.modaps.eosdis.nasa.gov/active\\_fire/](https://firms.modaps.eosdis.nasa.gov/active_fire/). MOPITT CO data can be downloaded from  
412 <https://asdc.larc.nasa.gov/project/MOPITT>. MERRA-2 data are available online through the  
413 NASA Goddard Earth Sciences Data Information Services Center (GES DISC;  
414 <https://disc.gsfc.nasa.gov>).

#### 415 **Acknowledgments**

416 The work is primarily supported by the Ministry of Science and Technology, Taiwan under grants  
417 MOST 110-2811-M-008-562 and MOST 109-2811-M-008-553. The authors would like to  
418 acknowledge Environmental Protection Administration (EPA) Taiwan for supporting air  
419 pollutants monitoring at Lulin Atmospheric Background Station (LABS, 23.47°N 120.87°E, 2862  
420 m MSL). The authors thank NASA and NOAA for providing MOPITT and MODIS satellite data.  
421 We thank NASA's Global Monitoring and Assimilation Office (GMAO) for providing the  
422 Modern-Era Retrospective analysis for Research and Applications, Version 2 (MERRA-2) data.

#### 423 **References**

424 Bond, T. C., Streets, D. G., Yarber, K., Nelson, S., Woo, J., & Klimont, Z. (2004). A technology-  
425 based global inventory of black and organic carbon emissions from combustion. *Journal of*  
426 *Geophysical Research*, 109(D14), D14203. <https://doi.org/10.1029/2003JD003697>

427 Bond, T. C., Doherty, S. J., Fahey, D. W., Forster, P. M., Berntsen, T., DeAngelo, B. J., et al.  
428 (2013). Bounding the role of black carbon in the climate system: A scientific assessment.  
429 *Journal of Geophysical Research: Atmospheres*, 118(11), 5380– 5552.  
430 <https://doi.org/10.1002/jgrd.50171>

- 431 Buchard, V., Randles, C. A., Da Silva, A. M., Darmenov, A., Colarco, P. R., Govindaraju, R., et  
432 al. (2017). The MERRA-2 aerosol reanalysis, 1980 onward, Part II: Evaluation and case studies.  
433 *Journal of Climate*, 30(17), 6851– 6872. <https://doi.org/10.1175/JCLI-D-16-0613.1>
- 434 Chen, S., Olofsson, P., Saphangthong, T., & Woodcock, C.E. (2023). Monitoring shifting  
435 cultivation in Laos with Landsat time series. *Remote Sensing of Environment*, Volume 288,  
436 2023,113507. <https://doi.org/10.1016/j.rse.2023.113507>
- 437 Chuang, M.-T., Fu, J. S., Lee, C.-T., Lin, N.-H., Gao, Y., Wang, S.-H., Sheu, G.-R., Hsiao, T.-C.,  
438 Wang, J.-L., & Yen, M.-C. (2015). The simulation of long-range transport of biomass burning  
439 plume and short-range transport of anthropogenic pollutants to a mountain observatory in East  
440 Asia during the 7-SEAS/2010 Dongsha Experiment. *Aerosol and Air Quality Research*, 16(11),  
441 2933– 2949. <https://doi.org/10.4209/aaqr.2015.07.0440>
- 442 Deeter, M. N., Edwards, D. P., Francis, G. L., Gille, J. C., Mao, D., Martínez-Alonso, S., et al.  
443 (2019). Radiance-based retrieval bias mitigation for the MOPITT instrument: The version 8  
444 product. *Atmospheric Measurement Techniques*, 12, 4561– 4580. [https://doi.org/10.5194/amt-](https://doi.org/10.5194/amt-12-4561-2019)  
445 [12-4561-2019](https://doi.org/10.5194/amt-12-4561-2019)
- 446 Ding, K., Huang, X., Ding, A. J., Wang, M. H., Su, H., Kerminen, V. M., et al. (2021). Aerosol-  
447 boundary-layer-monsoon interactions amplify semi-direct effect of biomass smoke on low  
448 cloud formation in Southeast Asia. *Nature Communications*, 12(1), 6416.  
449 <https://doi.org/10.1038/s41467-021-26728-4>
- 450 Gelaro, R., McCarty, W., Suárez, M. J., Todling, R., Molod, A., Takacs, L., Randles, C. A., et al.  
451 (2017). The Modern-Era Retrospective Analysis for Research and Applications, Version 2  
452 (MERRA-2). *Journal of Climate*, 30, 5419–5454. <https://doi.org/10.1175/jcli-d-16-0758.1>
- 453 Giglio, L., Randerson, J. T., & van der Werf, G. R. (2013). Analysis of daily, monthly, and annual  
454 burned area using the fourth-generation global fire emissions database (GFED4). *Journal of*  
455 *Geophysical Research: Biogeosciences*, 118(1), 317– 328. <https://doi.org/10.1002/jgrg.20042>
- 456 Giglio, L., Boschetti, L., Roy, D. P., Humber, M. L., & Justice, C. O. (2018). The Collection 6  
457 MODIS burned area mapping algorithm and product. *Remote Sensing of Environment*, 217, 72–  
458 85. <https://doi.org/10.1016/j.rse.2018.08.005>

- 459 Hsiao, T. C., Ye, W. C., Wang, S. H., Tsay, S. C., Chen, W. N., Lin, N. H., et al. (2016).  
460 Investigation of the CCN activity, BC and UVBC mass concentrations of biomass burning  
461 aerosols during the 2013 BASELInE campaign. *Aerosol and Air Quality Research*, 16(11),  
462 2742–2756. <https://doi.org/10.4209/aaqr.2015.07.0447>
- 463 Hoesly, R. M., Smith, S. J., Feng, L., Klimont, Z., Janssens-Maenhout, G., Pitkanen, T., Seibert,  
464 J. J., Vu, L., Andres, R. J., Bolt, R. M., Bond, T. C., Dawidowski, L., Kholod, N., Kurokawa,  
465 J.-i., Li, M., Liu, L., Lu, Z., Cecilia, M., Moura, P., O'Rourke, P. R., & Zhang, Q. (2018).  
466 Historical (1750–2014) anthropogenic emissions of reactive gases and aerosols from the  
467 community emissions data system (CEDS). *Geoscientific Model Development (Online)*, 11,  
468 369–408. <https://doi.org/10.5194/gmd-11-369-2018>
- 469 Hou, O, S. X., & Orth, R. (2020). Observational evidence of wildfire-promoting soil moisture  
470 anomalies. *Scientific Reports*, 10, 11008. <https://doi.org/10.1038/s41598-020-67530-4>
- 471 Huang, W. R., Wang, S. H., Yen, M. C., Lin, N. H., & Promchote, P. (2016). Interannual variation  
472 of springtime biomass burning in Indochina: Regional differences, associated atmospheric  
473 dynamical changes, and downwind impacts. *Journal of Geophysical Research: Atmospheres*,  
474 121, 10,016–10,028. <https://doi.org/10.1002/2016JD025286>
- 475 Huang, H.-Y., Wang, S.-H., Huang, W.-X., Lin, N.-H., Chuang, M.-T., Da Silva, A. M., & Peng,  
476 C.-M. (2020). Influence of synoptic-dynamic meteorology on the long-range transport of  
477 indochina biomass burning aerosols. *Journal of Geophysical Research: Atmospheres*, 125(3),  
478 e2019JD031260. <https://doi.org/10.1029/2019JD031260>
- 479 Huffman, G., Behrangi, A., Bolvin, D., & Nelkin, E. (2022). GPCP Version 3.2 Satellite-Gauge  
480 (SG) Combined Precipitation Data Set, Edited by Huffman, G.J., Behrangi, A., Bolvin, D.T.,  
481 Nelkin, E.J., Greenbelt, Maryland, USA, Goddard Earth Sciences Data and Information  
482 Services Center (GES DISC). <https://doi.org/10.5067/MEASURES/GPCP/DATA304>
- 483 IPCC. (2021). Climate change 2021: The physical science basis. In V. Masson-Delmotte, et al.  
484 (Eds.), *Contribution of Working Group I to the Sixth Assessment Report of the*  
485 *Intergovernmental Panel on Climate Change*. Cambridge University Press.

- 486 Jainontee, K., Pongkiatkul, P., Wang, Y.L., Weng, R.J.F., Lu, Y.T., Wang, T.S., Chen, W.K.  
487 (2023). Strategy Design of PM<sub>2.5</sub> Controlling for Northern Thailand. *Aerosol and Air Quality*  
488 *Research*. 23, 220432. <https://doi.org/10.4209/aaqr.220432>
- 489 Kendall, M. G. (1975). Rank Correlation Methods. New York, NY: Oxford University Press.
- 490 Lee, C.-T., Ram, S. S., Nguyen, D. L., Chou, C. C., Chang, S.-Y., Lin, N.-H., Chang, S.-C., Hsiao,  
491 T.-C., Sheu, G.-R., & Ou-Yang, C.-F. (2016). Aerosol chemical profile of near-source biomass  
492 burning smoke in Sonla, Vietnam during 7-SEAS campaigns in 2012 and 2013. *Aerosol and*  
493 *Air Quality Research*, 16(11), 2603– 2617. <https://doi.org/10.4209/aaqr.2015.07.0465>
- 494 Li, J., Hann, Z., Surapipith, V., Fan, W., Thongboonchoo, N., Wu, J., Li, J., Tao, J., Wu, Y.,  
495 Macatangay, R., Bran, S.H., Yu, E., Zhang, A., Liang, L., Zhang, R. (2022). Direct and indirect  
496 effects and feedbacks of biomass burning aerosols over Mainland Southeast Asia and South  
497 China in springtime. *Science of the Total Environment*. 842, 156949.  
498 <https://doi.org/10.1016/j.scitotenv.2022.156949>
- 499 Lin, C. Y., H. M. Hsu, Y. H. Lee, C. H. Kuo, Y. F. Sheng, & Chu, D. A. (2009). A new transport  
500 mechanism of biomass burning from Indochina as identified by modeling studies. *Atmospheric*  
501 *Chemistry and Physics*, 9, 7901–7911. <https://doi.org/10.5194/acp-9-7901-2009>
- 502 Lin, N.-H., Tsay, S. C., Maring, H. B., Yen, M. C., Sheu, G. R., Wang, S. H., Chi, K. H., Chuang,  
503 M. T., Ou-Yang, C. F., Fu, J. S., Reid, J. S., Lee, C. T., Wang, L. C., Wang, J. L., Hsu, C. N.,  
504 Sayer, A. M., Holben, B. N., Chu, Y. C., Nguyen, X. A., Sopajaree, K., Chen, S. J., Cheng, M.  
505 T., Tsuang, B. J., Tsai, C. J., Peng, C. M., Schnell, R. C., Conway, T., Chang, C. T., Lin, K. S.,  
506 Tsai, Y. I., Lee, W. J., Chang, S. C., Liu, J. J., Chiang, W. L., Huang, S. J., Lin, T. H., & Liu,  
507 G. R. (2013). An overview of regional experiments on biomass burning aerosols and related  
508 pollutants in Southeast Asia: From BASE-ASIA and the Dongsha experiment to 7-SEAS.  
509 *Atmospheric Environment*, 78(0), 1– 19. <https://doi.org/10.1016/j.atmosenv.2013.04.066>
- 510 Lin, C. C., Chen, W. N., Loftus, A. M., Lin, C. Y., Fu, Y. T., Peng, C. M. and Yen, M. C.:  
511 Influences of the long-range transport of biomass-burning pollutants on surface air quality  
512 during 7-SEAS field campaigns. *Aerosol and Air Quality Research*, 17(10), 2595–2607.  
513 <https://doi.org/10.4209/aaqr.2017.08.0273>

- 514 Mann, H. B. (1945). Nonparametric tests against trend. *Econometrica*, 13, 245–259.  
515 doi:10.2307/1907187
- 516 Messerli, P., Heinimann, A., Epprecht, M. (2009). Finding homogeneity in heterogeneity - a new  
517 approach to quantifying landscape mosaics developed for the Lao PDR. *Human Ecology*, 37,  
518 291–304. <https://doi.org/10.1007/s10745-009-9238-1>
- 519 Murray, C.J., Aravkin, A.Y., Zheng, P., Abbafati, C., Abbas, K.M., Abbasi-Kangevari, M., et al.,  
520 (2020). Globalburdenof87risk factors in 204 countries and territories, 1990–2019: a systematic  
521 analysis for the global burden of disease study 2019. *Lancet* (10258), 1223–1249.  
522 [https://doi.org/10.1016/S0140-6736\(20\)30752-2](https://doi.org/10.1016/S0140-6736(20)30752-2)
- 523 Nguyen, G.T.H., Nguyen, T.T.T., Shimadera, H., Uranishi, K., Matsuo, T., Kondo, A. (2022).  
524 Estimating Mortality Related to O3 and PM2.5 under Changing Climate and Emission in  
525 Continental Southeast Asia. *Aerosol and Air Quality Research*, 22, 220105.  
526 <https://doi.org/10.4209/aaqr.220105>
- 527 Ou-Yang, C. F., Ravindra Babu, S., Jia-Ren Lee, Ming-Cheng Yen, Stephen M. Griffith, Chia-  
528 Ching Lin, Shuenn-Chin Chang and Neng-Huei Lin. (2022). Detection of stratospheric  
529 intrusion events and their role in ozone enhancement at a mountain background site in sub-  
530 tropical East Asia. *Atmospheric Environment*, 268, 118779,  
531 <https://doi.org/10.1016/j.atmosenv.2021.118779>
- 532 Pan, X., Ichoku, C., Chin, M., Bian, H., Darmenov, A., & Colarco, P. (2020). Six global biomass  
533 burning emission datasets: Intercomparison and application in one global aerosol model.  
534 *Atmospheric Chemistry and Physics*, 20(2), 969–994. <https://doi.org/10.5194/acp-20-969-2020>
- 535 Pani, S. K., Wang, S.-H., Lin, N.-H., Lee, C.-T., Tsay, S.-C., Holben, B. N., Janjai, S., Hsiao, T.-  
536 C., Chuang, M.-T., Chantara, S. (2016). Radiative effect of springtime biomass-burning  
537 aerosols over northern Indochina during 7-SEAS/BASELInE 2013 campaign. *Aerosol and Air*  
538 *Quality Research*, 16, 2802-2817. <https://doi.org/10.4209/aaqr.2016.03.0130>
- 539 Pani, S. K., Lin, N. H., Chantara, S., Wang, S. H., Khamkaew, C., Prapamontol, T. Janjai, S.  
540 (2018). Radiative response of biomass-burning aerosols over an urban atmosphere in northern

- 541 peninsular Southeast Asia. *Science of the Total Environment*, 633, 892–911.  
542 <https://doi.org/10.1016/j.scitotenv.2018.03.204>
- 543 Ravindra Babu, S., Nguyen, L. S. P., Sheu, G.-R., Griffith, S. M., Pani, S. K., Huang, H.-Y., and  
544 Lin, N.-H. (2022) Long-range transport of La Soufrière volcanic plume to the western North  
545 Pacific: Influence on atmospheric mercury and aerosol properties. *Atmospheric Environment*,  
546 268, 118806. <https://doi.org/10.1016/j.atmosenv.2021.118806>
- 547 Reid, J. S., Hyer, E. J., Johnson, R., Holben, B. N., Yokelson, R. J., Zhang, J., Campbell, J. R. et  
548 al. (2013). Observing and understanding the Southeast Asian aerosol system by remote sensing:  
549 An initial review and analysis for the Seven Southeast Asian Studies (7SEAS) program.  
550 *Atmospheric Research*, 122, 403-468. <https://doi.org/10.1016/j.atmosres.2012.06.005>
- 551 Rodell, M., Houser, P. R., Jambor, U., Gottschalck, J., Mitchell, K., Meng, C.-J., Arsenault, K.,  
552 Cosgrove, B., et al., (2004). The Global Land Data Assimilation System. *Bulletin of the*  
553 *American Meteorological Society*. Vol. 85, No. 3, pp. 381-394. DOI: 10.1175/BAMS-85-3-381  
554 ISSN: 0003-0007, 1520-0477
- 555 Tsay, S.-C., Maring, H. B., Lin, N. H., Buntoung, S., Chantara, S., Chuang, H. C., Wiriya, W.,  
556 Yen, M. C., et al. (2016). Satellite-surface perspectives of air quality and aerosol-cloud effects  
557 on the environment: An overview of 7-SEAS/BASELInE. *Aerosol and Air Quality Research*,  
558 16(11), 2581– 2602. <https://doi.org/10.4209/aaqr.2016.08.0350>
- 559 Thao, N.N.L., Pimonsree, S., Prueksakorn, K., Thao, P.T.B., Vongruang, P. (2022). Public health  
560 and economic impact assessment of PM2.5 from open biomass burning over countries in  
561 mainland Southeast Asia during the smog episode. *Atmospheric Pollution Research*, 13 (6),  
562 101418. <https://doi.org/10.1016/j.apr.2022.101418>.
- 563 United Nations Environment Programme (2021). *Regulating Air Quality: The first Global*  
564 *Assessment of Air Pollution Legislation*. Nairobi.
- 565 Vadrevu, K. P., Lasko, L. Giglio, C. Justice. (2015). Vegetation fires, absorbing aerosols and  
566 smoke plume characteristics in diverse biomass burning regions of Asia. *Environmental*  
567 *Research Letters*, 10 (2015), 105003. <https://doi.org/10.1088/1748-9326/10/10/105003>

- 568 Vadrevu, K. P., Lasko, K., Giglio, L., Schroeder, W., Biswas, S., and? Justice, C. (2019). Trends  
569 in vegetation fires in South and Southeast Asian countries. *Scientific Reports*, 9(1), 7422.  
570 <https://doi.org/10.1038/s41598-019-43940-x>
- 571 van der Werf, G. R., Randerson, J. T., Giglio, L., van Leeuwen, T. T., Chen, Y., Rogers, B. M.,  
572 Mu, M., van Marle, M. J. E., Morton, D. C., Collatz, G. J., Yokelson, R. J., and Kasibhatla, P.  
573 S. (2017). Global fire emissions estimates during 1997–2016, *Earth Systems Sciences Data*, 9,  
574 697–720. <https://doi.org/10.5194/essd-9-697-2017>
- 575 van Marle, M. J. E., Kloster, S., Magi, B. I., Marlon, J. R., Daniiau, A.-L., Field, R. D., Arneth, A.,  
576 Forrest, M., Hantson, S., Kehrwald, N. M., Knorr, W., Lasslop, G., Li, F., Mangeon, S., Yue,  
577 C., Kaiser, J. W., van der Werf, G. R. (2017). Historic global biomass burning emissions for  
578 CMIP6 (BB4CMIP) based on merging satellite observations with proxies and fire models  
579 (1750–2015), *Geoscience Model Development*, 10, 3329–3357. [https://doi.org/10.5194/gmd-  
580 10-3329-2017](https://doi.org/10.5194/gmd-10-3329-2017)
- 581 Yang, S., Wu, R., Jian, M., Huang, J., Hu, X., Wang, Z., Jiang, X. (2021). Climate change in  
582 Southeast Asia and surrounding areas. In: *Climate change in Southeast Asia and surrounding  
583 areas*. Science Press, Beijing and Springer Nature, Singapore, pp. 1–420. doi:10.1007/978-981-  
584 15-8225-7\_1.
- 585 Yang, S., Lau, W. K. M., Ji, Z., Dong, W., Yang, S. (2022). Impacts of radiative effect of pre-  
586 monsoon biomass burning aerosols on atmospheric circulation and rainfall over Southeast Asia  
587 and southern China, *Climate Dynamics*, 59, 417–432. [https://doi.org/10.1007/s00382-021-  
588 06135-7](https://doi.org/10.1007/s00382-021-06135-7)
- 589 Yabueng, N., Wiriya, W., Chantara, S. (2020). Influence of zero-burning policy and climate  
590 phenomena on ambient PM<sub>2.5</sub> patterns and PAHs inhalation cancer risk during episodes of  
591 smoke haze in Northern Thailand. *Atmospheric Environment*. 232, 117485.  
592 <https://doi.org/10.1016/j.atmosenv.2020.117485>